Available online at www.sciencedirect.com
ScienceDirect
Ceramics International 37 (2011) 207–214
CERAMICS INTERNATIONAL
www.elsevier.com/locate/ceramint

# Interface states and MWS polarization contributions to the dielectric response of low voltage ZnO varistor

C. Tsonos [a,*], A. Kanapitsas [a], D. Triantis [b], C. Anastasiadis [b], I. Stavrakas [b], P. Pissis [c], E. Neagu [d]

[a] Department of Electronics, Technological Educational Institute of Lamia, 35100 Lamia, Greece
[b] Department of Electronics, Technological Educational Institution of Athens, 12210 Athens, Greece
[c] Physics Department, Technical University of Athens, Zografou Campus, 15780 Athens, Greece
[d] Department of Physics, Technical University of Iasi, Mangeron 67, Iasi 700050, Romania

Received 18 June 2010; received in revised form 15 July 2010; accepted 22 August 2010
Available online 29 September 2010

**Abstract**

The main purpose of this work is to study the dielectric response of commercial low voltage ZnO varistors by means of dielectric relaxation spectroscopy (DRS) and thermally stimulated depolarization currents (TSDC) in a wide temperature range. Four relaxation processes have been studied here and all of them demonstrate Cole–Davidson behaviour. The first two faster relaxation mechanisms are known processes in ZnO varistors and those are related to the ZnO bulk traps. The next one faster relaxation mechanism attributed to the MWS polarization which should be related to the intergranular Bi-rich microregions. The remaining slower relaxation mechanism is associated to the grain boundaries interfaces. Based on the block model for the ZnO varistor a gradual reduction in the total depletion width is observed at a temperature about 330 K, which can be considered that is due to the gradual decrease of the interface states density at this temperature region.


*Keywords:* B. Grain boundaries; B. Interfaces; C. Dielectric properties; D. ZnO

## 1. Introduction

The zinc oxide (ZnO) varistor is a multi-phase component electronic ceramic device with nonlinear current–voltage (*I–V*) characteristic. ZnO-based varistors have become technologically important because of their highly nonlinear electrical characteristics, the applications of which include voltage stabilization transient surge suppression in electronic circuits and electronic power systems [1]. Varistors are available to protect circuits over a very wide range of voltages, from a few volts for low-voltage varistors in semiconductor circuits to tens of kilovolts for electrical power distribution networks. It is composed mainly of ZnO and other minor additions of various cationic oxides and it exhibits n-type semiconductor behaviour. The additives control grain sizes, grain resistivity and ZnO stability (the nonlinear behaviour is dramatically improved) [2,3]. Also, the microstructural homogeneity plays an important role for the ZnO stability [4]. The nonlinear current–voltage (*I–V*) characteristic is attributed to the back-to-back double Schottky barriers formed across the grain boundaries. Charge carriers are trapped inside the thin interface boundaries, between neighbour ZnO grains, and they are balanced by space charge regions at the adjacent zone of the grains in the double Schottky barrier configuration [2]. The pre-breakdown region (low-current linear region) is highly temperature dependent and it is determined by the impedance of grain boundaries [5]. The intermediate nonlinear region (breakdown region) is the most important feature of the ZnO varistor in which the device conducts large amount of current for small increase in voltage, and this phenomenon is almost independent of temperature [5]. The upturn region is controlled by the impedance of ZnO grains [6]. The breakdown phenomenon is still under debate and several models have been suggested such as the tunnelling model and the hot-electrons model [7,8].

There are two kinds of electron traps of special importance in ZnO varistors. The interface traps, situated at the boundary between ZnO–ZnO grains, and the bulk traps which arise from

* Corresponding author. Tel.: +30 2231060277; fax: +30 2231033945.
*E-mail address:* tsonos@teilam.gr (C. Tsonos).

0272-8842/$36.00 
doi:10.1016/j.ceramint.2010.08.036

donor-like traps in the bulk of ZnO grains. The varistor's function arises as a result of the presence of the depletion layers (interfaces) between adjacent ZnO grains. The oxygen is observed to be present at the grain boundary interfaces in excess as well, and plays an important role in the creation of the barrier height [6] as well as to the degradation and re-creation of potential barriers [9]. Removing the oxygen from the interfaces reduces the barrier height and increases the leakage currents. The main microscopic constituents of ZnO varistor materials are ZnO grains, spinel grains, and bismuth-rich intergranular phases [10].

Electronic transitions in semiconductors between localised levels in the forbidden gap or between localised levels and the free bands are in every way equivalent to dipolar rotations, in that they result in sudden displacement of charge [11]. Therefore, the dielectric relaxation spectroscopy (DRS) is a convenient method to detect electronic transitions in ZnO varistor. When DRS measurements are performed below room temperature, it is expected to observe dielectric relaxation peaks arising from the dielectric response of bulk traps in ZnO [12,13]. Several works have been done in ZnO varistors, by means of DRS, which generally focused to the ZnO bulk traps characteristics and their dependence to the microstructure formation composition and/or dopants [13–17]. ZnO varistor as a multi-phase component material presents a high degree of heterogeneity. In heterogeneous systems the Maxwell–Wagner–Sillars (MWS) polarization is often present. However, to the best of our knowledge there has not been evidence for the MWS polarization detection in ZnO varistor until now. Also, above room temperatures the DC conductivity masks the contribution of interface states in the frequency spectrum of DRS measurements. Therefore the study of the interface states has not been made by means of DRS measurements, which should be given additional information for the ZnO varistor operation.

Apart from the DRS method, other characterization techniques such as deep level transient spectroscopy (DLTS), isothermal capacitance transient spectroscopy (ICTS) and current–voltage (*I–V*) measurements have been used as well, in order to investigate the ZnO varistor response of interface states and/or bulk traps in relation to their microstructure characteristic [18–21].

In a previous work we studied the dielectric response of low voltage ZnO varistor in an interesting narrow low temperature range [22]. Three relaxation processes were studied, exhibiting a very strong Cole–Davidson behaviour. The faster relaxation process shows an unusual thermal behaviour. Initially, its relaxation time increases as the temperature rises but later it becomes thermally activated. The transition temperature of thermal behaviour of this process was found very close to the characteristic value of $0.4\theta_D = 160$ K, where $\theta_D$ is the Debye temperature of ZnO. The de-activation energy of this process has been estimated by using the Arrhenius type relation to be 78 meV, a value very close to the higher longitudinal optical (LO) phonon energy in ZnO, 72 meV. These facts consist a strong indication that the predicted Holstein transition between large to small-polaron motion should be observed in ZnO. The two remaining relaxations are electronic processes; the slower one is associated with the doubly ionised zinc interstitial $Zn_i^{\bullet\bullet}$, while the other should be related to defects induced by the dopants, or of complexes of intrinsic native defect with dopant impurities.

In the present work we continue the study of the dielectric responses of low voltage ZnO varistors, at higher temperatures, by the means of dielectric relaxation spectroscopy (DRS) and thermally stimulated depolarization currents (TSDC). In the DRS measurements that we have made, we have used the complex dielectric constant formalism, $\varepsilon^*(f)$, of the experimental data which exhibit very high complexity. In the current literature, the analysis deals usually only with the apparent loss peaks of such device materials. Here, a detailed analysis has been made in the complex frequency spectrum by fitting a sum of the Havriliak–Negami expression. The results of the DRS measurements are discussed and compared to the TSDC measurements, in order to identify the role of interface states and MWS polarization to the dielectric response of ZnO varistors in a wide temperature and frequency range. Better knowledge, especially of the interface states influence in the dielectric response, it is a necessary prerequisite not only for improving the varistor's operation, but also to give new insights for understanding phenomena related to the grain boundary effects.

## 2. Experimental procedure

### 2.1. Sample preparation

The samples used in this work procured from commercial sources. The conventional ceramic pressing and liquid-phase sintering technique has been used for the fabrication of the samples. Powder of ZnO has been mixed with appropriate amounts of other oxides of Mn, Si, Bi, Sb, Al, Ni and Co. The powder mixture, which is contained about 96 mol% ZnO, was ball milled with alcoholic solution for 24 h. The resultant mixture was dried at 110 °C for 15 h and then it was pressed uniaxially into discs of 12 mm in diameter at a pressure 90 MPa. The discs were sintered at 1200 °C in air atmosphere for 1 h with heating and cooling rate of 7 °C/min. The final thickness of the samples was 0.9 mm. Silver paste was applied to the faces of the samples, which were subsequently heated at 600 °C for 20 min, to provide electrodes.

### 2.2. Methods characterization

In order to check the microstructure of the samples a JSM – 6300 (JEOL) Scanning Electron Microscope (SEM) was used with accelerator voltage 0.2–30 kV. SEM micrographs showed relatively high degree of non-uniformity. The average grain size was measured by the linear intercept method and found to be 20 μm. The dominant secondary phase is the bismuth-rich phase as expected because is known that the $Bi_2O_3$ is insoluble in the ZnO grains.

In order to justify the electrical characteristics of the samples, *I–V* measurements were carried out with a Keithley 6517 electrometer and a Keithley 617 programmable electrometer with a Hameg 814 power supply unit. The varistor

voltage $V_{1\ mA}$ was determined at current density 1 mA/cm$^2$ and was found to be 14 V/mm. The exponent $\alpha$ ($I = kV^{\alpha}$) was found to have relative large values, between 40 and 75 for values of current density varying from $10^{-9}$ A/cm$^2$ up to $10^{-2}$ A/cm$^2$.

DRS measurements were carried out isothermally in a broad frequency range. The sample was inserted between the gold-plated plates of the capacitor cell. A Novocontrol Alpha Analyser, in combination with the Novocontrol Quatro Cryosystem, was used for broadband DRS measurements in the frequency range $10^{-1}$ to $10^{6}$ Hz at a temperature range from 193 K up to 433 K.

For the TSDC measurements a Keithley 617 Electrometer in combination with the Novocontrol Quatro Cryosystem and a BDS TSDC cell were used. The sample was polarized at 300 K for 5 min and then cooled with rate 10 K/min down to 160 K. Afterwards without an applied voltage, it was heated at a rate of 4 K/min up to room temperature, 300 K, while the discharged current was recording continuously. The polarization voltages, which have been applied, correspond to the pre-breakdown and the upturn high-current regions of ZnO varistor sample.

## 3. Results and discussion

### 3.1. TSDC measurements

Fig. 1 shows TSDC plots for three different values of the polarizing electric field, $E_p = 75$ V/cm, $E_p = 150$ V/cm and $E_p = 300$ V/cm. The first peak corresponds to pre-switch $E$–$J$ characteristic linear region, while the other two to the high-current region of ZnO varistor. In both regions, two peaks are clearly observed, one at lower temperatures and the other one at higher temperatures. The two peaks are located at temperatures of about 235 K and 280 K respectively. The temperature of each peak, $T_m$, is almost unaffected by the value of the polarizing field $E_p$.

In Fig. 2 the maximum current $I_{max}$ of each peak is presented, after the background current subtraction, as a function of polarizing field $E_p$. The first two lower polarizing fields correspond to the pre-switch characteristic linear region

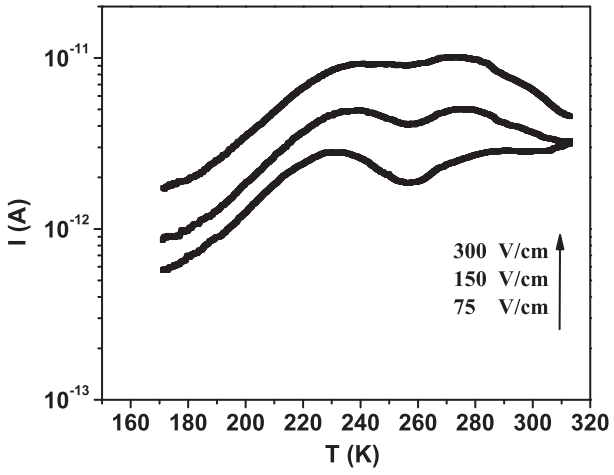


Fig. 1. TSDC plots for different values of the polarizing electric field $E_p$.

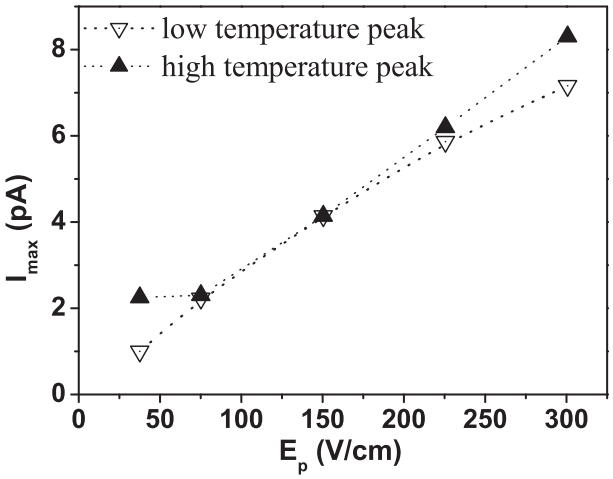


Fig. 2. The maximum current, $I_{max}$, of the TSDC peaks as a function of polarizing electric field $E_p$.

of ZnO varistor. This region is controlled from ZnO–ZnO grain boundary interfaces which present the highest resistivity. As we can observe in this diagram representing $I_{max}$ versus $E_p$, the maximum current of the higher temperature peak (slower mechanism) is almost unaffected for values of polarizing field correspond to the pre-switch linear region. This is the first evidence that such a mechanism should be related to the grain boundaries interface region. At higher values of the polarizing field, which correspond to the high-current region, $I_{max}$ gradually increases. The grain boundary interface regions, apart from controlling the DC conductivity, are characterized as well by the existence of the interfacial states and the empty electron traps in grains boundary layers. The interfacial states arise because the trapped electrons act as a sheet of negative charge at the boundary leaving behind a layer of positively charged donor sites on either side of the boundary [2,29]. Therefore, the higher temperature peak in TSDC measurements should be related to the interfacial states of trapped electrons and/or the empty electron traps at the boundaries between the ZnO grains.

The $I_{max}$ of the lower temperature peak (faster mechanism) in TSDC measurements, increases as the polarizing electric field rises. However, it presents a nonlinear behaviour and has a tendency for saturation at high fields. This behaviour is characteristic of Maxwell–Wagner–Sillars (MWS) polarization in heterogeneous systems [23,24]. MWS polarization is a relaxation process appearing in heterogeneous materials because of the accumulation of charges at the interfaces between microregions with different dielectric constants and conductivities. The phase of ZnO varistor with the above characteristics is the intergranular Bi-rich microregion which contains various ions during the varistor fabrication process. These microregions are characterized also by the presence of amorphous and crystalline phases [10]. Therefore, the lower temperature TSDC peak should be related to the intergranular Bi-rich microregions. It must be noted here that the contribution of the varistors porosity to this mechanism should not be excluded.

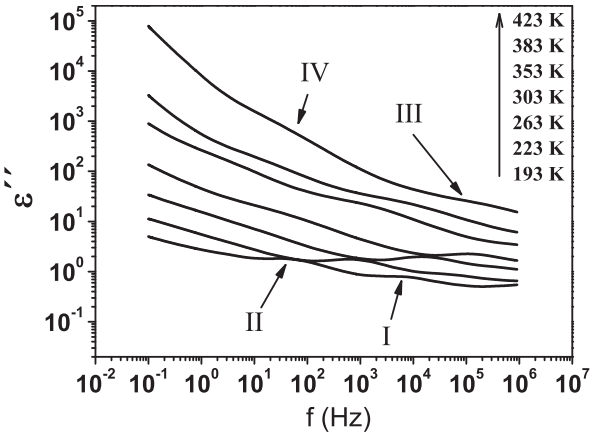


Fig. 3. The imaginary part, $\varepsilon''$, versus frequency, $f$, at various temperatures. Four relaxations appear in the frequency spectrum: I, II, III and IV in order from high to low frequencies region.

### 3.2. DRS measurements

Fig. 3 shows the variation in the imaginary part $\varepsilon''$, of the complex dielectric constant, $\varepsilon^*(f) = \varepsilon'(f) - i\varepsilon''(f)$, versus frequency $f$, at temperatures varying from 193 K up to 423 K. Four relaxations are present in the corresponding frequency range, which shift to higher frequencies as the temperature rises. Henceforth, the four relaxations are referred as I, II, III and IV in order of increasing the relaxation time $\tau$ ($\tau = 1/2\pi f_p$). Relaxation I shows up at higher frequencies while the relaxation IV appears at the lower frequencies. Above 373 K the DC conductivity is dominant in the low frequency region. The contribution of the DC conductivity on the dielectric loss $\varepsilon''$ is reciprocal to the frequency $f$, i.e. it corresponds to the linear segment of lower frequency range.

To resolve the contribution of each relaxation mechanism, the experimental data of Fig. 3 are fitted in terms of a sum of Havriliak–Negami (H–N) expression described by the following equation [25]

$$\varepsilon''(\omega) = A\omega^{-n} - \mathrm{Im}\sum_{k=1}^{2} \frac{\Delta\varepsilon'_k}{\left[1 + (i\omega\tau_{ok})^{(1-\alpha_k)}\right]^{\beta_k}}, \quad (1)$$

where Im represents the imaginary part of the expression. Parameters $\alpha$ ($0 \le \alpha < 1$) and $\beta$ ($0 < \beta \le 1$) describe the deviations from the simple relaxation time. When $\alpha = 0$ and $\beta = 1$ the H–N equations coincide with the respective Debye equation. $\Delta\varepsilon'_k$ is the contribution of each relaxation to the real part of the complex dielectric constant $\varepsilon^*$. $\tau_{ok} = 1/2\pi f_{ok}$ is a characteristic relaxation time parameter while $f_{ok}$ is the corresponding characteristic frequency that is closely related to each frequency, where the dielectric losses $\varepsilon''$ has a maximum, $f_p$.

At the higher temperature region, 303–373 K, the term $A\omega^{-n}$ represents the linear contribution of the DC conductivity to the dielectric losses spectra with value of $n = 1$, while the other two relaxations are the III and IV. At lower temperatures, below 300 K, the term $A\omega^{-n}$ represents the linear contribution of the relaxation III to the log–log frequency spectrum of dielectric losses, and the other two relaxations are the I and II. Parameter A defines the position while the parameter $n$, where $n = (1 - \alpha)\beta$, defines the slope of the linear right hand side contribution of relaxation III. All fits have been done using the non-linear least-squares Marquardt–Levenberg algorithm. Fig. 4 shows the best fittings of Eq. (1) at temperatures 233 K and 363 K. The values of the fitting parameters $\alpha$, $\beta$, $f_p$ and $\Delta\varepsilon'$ are given in Tables 1 and 2. All relaxation processes tend to exhibit a behaviour similar to the Cole–Davidson one. The deviation from the Debye response has been a subject that several authors have studied in depth. Fernandez Hevia et al. suggested that the dominance of deep over shallow donors in polycrystalline ZnO and other grain boundary semiconductors could explain the observed frequency and time-domain non-Debye behaviour [26]. Garcia-Belmonte et al. suggested that the observed non-Debye responses are associated to the density or to the disordered distribution of traps [27].

The Arrhenius plots of the maximum loss peak position, $f_p$, for all relaxation processes are depicted in Fig. 5. All the relaxations exhibit a thermal activated Arrhenius type behaviour

$$f_p = f_o e^{-E/kT}, \quad (2)$$

where $f_o$ is a pre-exponential factor, $E$ the activation energy, $k$ the Boltzmann constant and $T$ the temperature in K. Relaxation

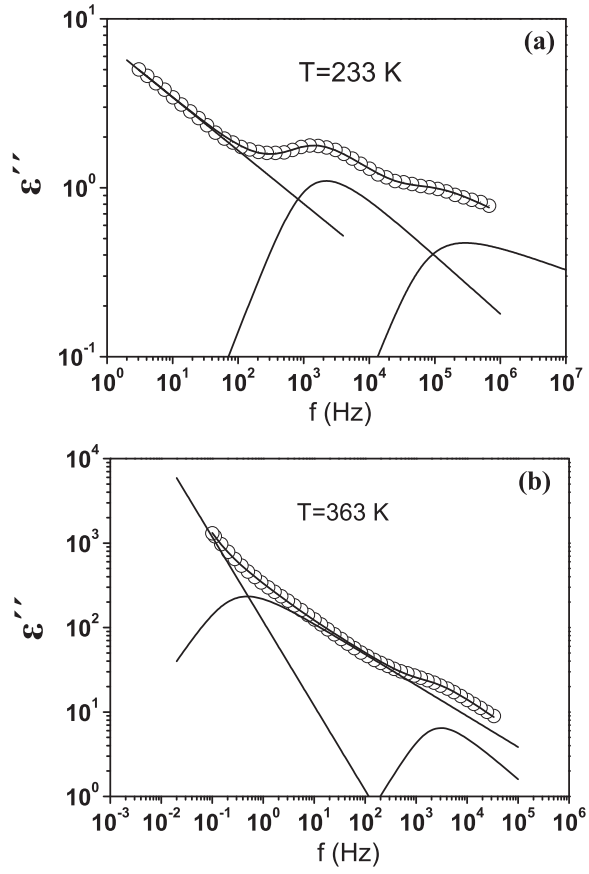


Fig. 4. Representative best fitting of Eq. (1) to the diagrams $\varepsilon''$ versus $f$ at 233 K (a) and 363 K (b). The lines represent the best fit according to Eq. (1) and the contribution of the each process to the total spectrum.

Table 1
Values of the fitting parameters $\alpha$, $\beta$ and $\Delta\varepsilon'$, of Eq. (1), for the relaxation processes I and II.

| $T$ (K) | Relaxation I | | | Relaxation II | | |
|---|---|---|---|---|---|---|
| | $\alpha$ | $\beta$ | $\Delta\varepsilon'$ | $\alpha$ | $\beta$ | $\Delta\varepsilon'$ |
| 193 | 0.05 | 0.19 | 2.8 | 0.13 | 0.50 | 6.0 |
| 213 | 0 | 0.18 | 2.3 | 0 | 0.36 | 5.8 |
| 233 | 0 | 0.14 | 3.2 | 0 | 0.35 | 4.0 |
| 253 | 0.03 | 0.15 | 3.8 | 0 | 0.40 | 5.9 |
| 273 | 0 | 0.16 | 3.0 | 0 | 0.33 | 7.0 |
| 293 | – | – | – | 0 | 0.26 | 9.6 |
| 313 | – | – | – | 0.08 | 0.31 | 6.5 |

IV presents a change in the slope at about 333 K. The activation energy of relaxation IV, as evaluated by using Eq. (2), was found to be $(0.73 \pm 0.03)$ eV below 333 K, while its value is $(0.19 \pm 0.02)$ eV above 333 K. The other three relaxations I, II and III have activation energies $(0.29 \pm 0.01)$ eV, $(0.37 \pm 0.01)$ eV and $(0.85 \pm 0.03)$ eV respectively.

The Arrhenius plots of Fig. 5, also include the TSDC measurements of lower and higher temperature peaks of Fig. 1. In TSDC measurements, at the peak temperature of a relaxation mechanism the equivalent frequency is equal to $f_{eq} = 1/2\pi\tau$, where $\tau$ is the time scale of TSDC measurements and has a value of about 100 s [24,28]. Therefore, the lower temperature TSDC peak located at 235 K has at this temperature equivalent frequency $f_{eq} = 1.6 \times 10^{-3}$ Hz, while the higher TSDC peak located at 280 K has also at this temperature the same equivalent frequency. The extrapolation of the linear fittings (Eq. (2)) of relaxations III and IV, is in very good agreement with the temperatures and frequencies position of the lower and higher temperature TSDC peaks respectively. This means that the relaxation III corresponds to the lower temperature TSDC peak, while the relaxation IV corresponds to the higher temperature TSDC peak of Fig. 1.

The general junction semiconductor theory, based on Debye-like dielectric responses, correlates the relaxation frequency $f_p$, $\omega_p = 2\pi f_p$, to the temperature, $T$, via the following relationship [29]

$$\omega_p = 2\pi f_p = \tau^{-1} = e_n = \sigma_n v_{th} N_c \exp\left(-\frac{\Delta E}{kT}\right), \quad (3)$$

Table 2
Values of the fitting parameters $\alpha$, $\beta$ and $\Delta\varepsilon'$, of Eq. (1), for the relaxation processes III and IV.

| $T$ (K) | Relaxation III | | | Relaxation IV | | |
|---|---|---|---|---|---|---|
| | $\alpha$ | $\beta$ | $\Delta\varepsilon'$ | $\alpha$ | $\beta$ | $\Delta\varepsilon'$ |
| 303 | 0.21 | 0.42 | 23 | 0 | 0.41 | 418 |
| 313 | 0.29 | 0.48 | 33 | 0 | 0.44 | 403 |
| 323 | 0.27 | 0.53 | 32 | 0.03 | 0.45 | 480 |
| 333 | 0.08 | 0.38 | 29 | 0 | 0.41 | 507 |
| 343 | 0 | 0.43 | 51 | 0 | 0.38 | 626 |
| 353 | 0 | 0.55 | 17 | 0.03 | 0.38 | 746 |
| 363 | 0 | 0.52 | 18 | 0.11 | 0.41 | 850 |
| 373 | – | – | – | 0.03 | 0.32 | 926 |

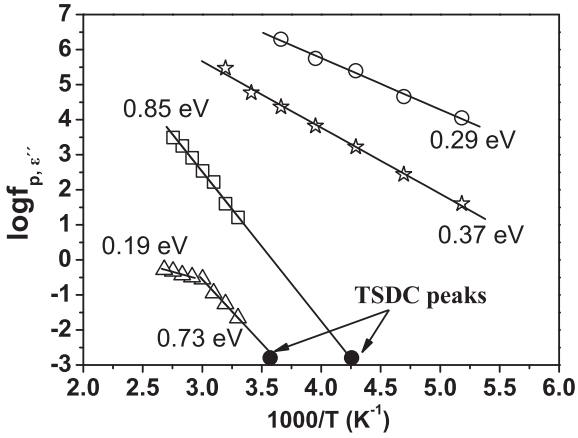


Fig. 5. Arrhenius plots of the four relaxations. In this figure we have included two points corresponding to the TSDC peaks of Fig. 1.

where $\tau$ is the time of the electron transition, $e_n$ is the characteristic emission rate, $\sigma_n$ the capture cross-section of the trapping states, $v_{th}$ the free-electron thermal velocity, $N_c$ is the density of states and $\Delta E$ is the energy difference between the conduction band and the trapping level. For a deep bulk donor in ZnO varistor the following relation stands [12,13]

$$\sigma_n v_{th} N_c = \frac{2g\sigma_n A^* T^2}{e}, \quad (4)$$

where $g$ is the spin degeneracy factor (equal to 0.5), $A^*$ is the effective Richardson's constant with a value of about 30 A cm$^{-2}$ K$^{-2}$ for ZnO, and $e$ is the electronic charge. If we assume that the capture cross-section is temperature independent, the slope of diagrams $\log(f_p/T^2)$ versus $1/T$ give the energy $\Delta E$, while the intercept is proportional to the capture cross-section $\sigma_n$. The plots $\log(f_p/T^2)$ versus $1/T$ in Fig. 6 yield values for energy $(0.26 \pm 0.01)$ eV and $(0.35 \pm 0.01)$ eV for the relaxations I and II respectively. For both relaxations, I and II, the capture cross-section have values $5 \times 10^{-14}$ cm$^2$ and $3 \times 10^{-14}$ cm$^2$ respectively. Even if the relaxations I and II are non-Debye and this means that the capture cross-section is a distributed parameter, nevertheless these values can be considered as a mean value, which is reasonable for the electron traps in semi-conducting materials [13,30].

Similar values of activation energies were found also for other different ZnO varistor systems, by using dielectric relaxation

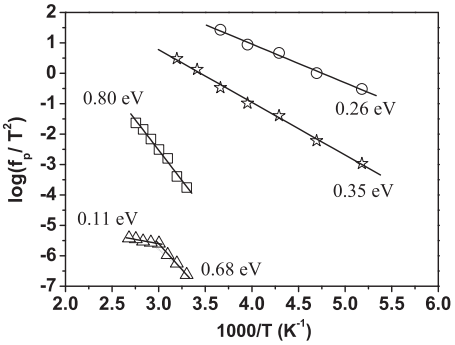


Fig. 6. Plots corresponding to Eqs. (3) and (4).

spectroscopy [13–17,31]. The relaxation I has activation energy very close to the second ionisation energy for zinc ion, which was estimated to be in the range 0.20–0.26 eV [13–17]. Thus, the relaxation I should be related with the doubly ionised zinc interstitial $Zn_i^{\bullet\bullet}$. On the other hand, the singly ionised oxygen vacancy has an energy level around 0.35 eV below the conduction band [15–17]. This means that the relaxation II should be associated with the oxygen vacancy $V_o^{\bullet}$.

The energy level for the relaxation III, was found to be $(0.80 \pm 0.03)$ eV according to Eq. (3), while the capture cross-section has been estimated to be $8 \times 10^{-9}$ cm$^2$. This large value of the capture cross-section, is out of the range for an electron trap and also is higher than that of the coulombic attractive centres, $\sim 10^{-11}$ cm$^2$ [32]. It must be noted also the significant large values of dielectric strength $\Delta\varepsilon'$ of relaxation III against the electronic transitions I and II (Tables 1 and 2). This suggests that the relaxation III should not be related to known electronic processes and supports the first opinion, from TSDC measurements, that may be related to the MWS polarization which take place at the intergranular Bi-rich microregions.

In higher voltage commercial ZnO varistors, a sudden drop of the potential barrier width has been observed at temperatures $T > 320$ K [19]. Such a change is expected to influence relaxation processes which are related to these regions. Relaxation IV presents a change in the slope at about 333 K as well. This is the second evidence that the relaxation IV should be related to the grain boundaries interface region.

Relaxation IV presents values of energy level and capture cross-section, $(0.68 \pm 0.03)$ eV and $2 \times 10^{-15}$ cm$^2$ respectively, below 333 K. The value of capture cross-section is reasonable for the electron traps in semiconducting materials. Gambino et al. [33] have reported the presence of interfacial states at 0.6–0.7 eV below the conduction band, in both bismuth- and praseodymium-doped ZnO. Other researchers, based on both DLTS and admittance spectroscopy, suggested that the interfacial states are somewhat higher from the above energy value, but lower than 1 eV below the conduction band [2,6,34]. Thus, the energy level $(0.68 \pm 0.03)$ eV is close to the one referred in the literature for the interfacial states.

Above 333 K, the relaxation IV presents values of energy level and capture cross-section, $(0.11 \pm 0.01)$ eV and $4 \times 10^{-24}$ cm$^2$ respectively. The value of capture cross-section is extraordinarily small for electronic transitions, and significantly smaller than that corresponding to coulombic repulsive centres, $\sim 10^{-21}$ cm$^2$ [32]. This indicates that Eq. (3), which is based on thermionic emission effect, it might be unable to describe electronic transitions in the grain boundary regions, at least above 330 K in ZnO varistor. Other processes should be taken into account such as thermally activated tunnelling effects [2,6]. According to Alim et al. [19] under low DC applied electric field, the electrons crossed over the forward side barrier and flow into the grain boundary layers. These electrons fill into the empty electron traps first and form space charges in the intergranular regions (grain boundary layers). These space charges can easily overcome the reverse side barrier because the barrier height is in low order and found to be smaller than 0.2 eV. This is in accordance to the energy level $(0.11 \pm 0.01)$ eV which we estimated for the relaxation IV above 333 K.

Based on the analysis presented above, we can conclude that the change in slope of IV process at 333 K, should be related to the change of the nature of this relaxation. Below 333 K the interfacial states contribution dominates, while above 333 K the empty electron traps within the grain boundary layers is the dominant one.

Let us consider now a simple model for the ZnO varistor, the block model [29]. The thickness of insulating dielectric which is lying between the sample electrodes is $Dt/d$, being $D$ the sample thickness, $t$ is the total depletion width of the back-to-back Schottky barrier (including the insulating barrier) and $d$ is the average of the ZnO conducting grains, about 20 μm for our materials. Since $t \ll d$, the volume between the electrodes is largely occupied by the conducting ZnO grains. If $k$ is the dielectric constant of the ZnO grains in the depletion layers, which has a value 8.5, it is expected that the capacitance of ZnO varistor sample is given by the following relation [29]

$$C = k\varepsilon_o \frac{A}{(Dt/d)} = \frac{d}{t} k\varepsilon_o \frac{A}{D}. \quad (5)$$

Therefore the static dielectric constant, $\varepsilon_s$, of the ZnO varistor sample is given by

$$\varepsilon_s = \frac{C}{C_o} = \frac{kd}{t}, \quad (6)$$

where $C_o$ is the geometrical capacitance of empty electrodes. If we add the strengths $\Delta\varepsilon'$ of the relaxations III and IV to the value of $\varepsilon'$ at 1 MHz, we get the value of the static dielectric constant $\varepsilon_s$, at each temperature. At a frequency of 1 MHz all the other processes have been relaxed and therefore were contributed to the real part of dielectric constant $\varepsilon'$. Based on the values of Table 2 and using Eq. (6), we can estimate the total depletion width $t$. The dependence of $t$ as a function of temperature is given in Fig. 7. A gradual reduction in total depletion width is observed at around 320 K. From a value of about 270 nm, up to 320 K, the total depletion width reduces to a value of about 150 nm up to 373 K. A similar observation has been made by Alim et al. [19]. They observed also a gradual

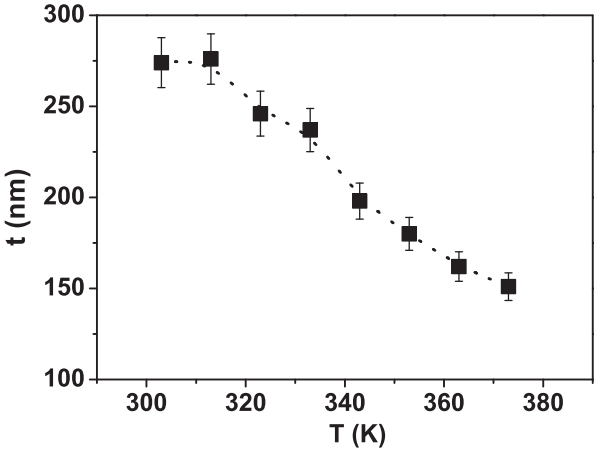


Fig. 7. The total depletion width, $t$, as a function of temperature, $T$.

reduction of the total depletion width from a value about 250 nm at 320 K, to a value of about 25 nm at around 370 K, by using low field *I–V* measurements in a higher voltage ZnO commercial varistor. From the macroscopic point of view, based on our DRS measurements, the reduction of the depletion width is due to the gradual increase of strength, $\Delta\varepsilon'$, of relaxation IV above 320 K.

In what follows, we will try to find the microscopic reason of the total depletion width reduction above 320 K. Let us consider the one back of the Schottky barrier. Assuming that the discrete nature of the charges can be ignored, the magnitude of the potential barrier can be calculated by solving the Poisson equation for the potential, $\Phi(x)$, from the knowledge of the grain boundary charge density $\rho(x)$ [2,35]

$$\frac{d^2\Phi(x)}{d^2x} = \frac{\rho(x)}{\varepsilon_r\varepsilon_o}, \tag{7}$$

where $\varepsilon_r$ is the dielectric constant of the depletion region and $\varepsilon_o$ the permittivity of free space. From the solution of Eq. (7) two important parameters can be extracted, the barrier height, $\Phi_B$, and the width of the depletion region, $d$, which both are given by the following relations

$$\Phi_B\,(V=0) = \frac{e^2 n_t}{8\varepsilon_r\varepsilon_o n_o} \tag{8}$$

and

$$d \approx \left(\frac{\varepsilon_r\Phi_B}{n_o}\right)^{1/2}, \tag{9}$$

where $n_t$ is the density of interfacial states, $n_o$ is the density of carrier concentration in the ZnO grains and $e$ is the electron charge. Substitution of $\Phi_B$ given by Eq. (8) into Eq. (9), leads to the next relation

$$t = 2d \propto \frac{n_t}{n_o}. \tag{10}$$

The concentration $n_o$ of ZnO bulk only slightly increases as the temperature rises, in the narrow temperature region of our interest 300–370 K, and has a value of about $\sim 10^{17}$ cm$^{-3}$ [36]. Therefore the gradual decreasing of the total depletion width, $t$, is related to the decrease of the interfacial states density, $n_t$, above 320 K.

As we have already mentioned earlier, the change in slope of IV process at around 330 K, should be related with the change of the nature of this relaxation. Below 330 K, the strength $\Delta\varepsilon'$ of the relaxation IV is almost constant and this leads to constant total depletion width with a value of about 270 nm (Fig. 7). The energy level of relaxation IV is close to the one referred in the literature for energy difference between conduction band and interfacial level. Also the value of capture cross-section is reasonable for the electron traps in semi-conducting materials. Therefore, in the relaxation IV below 330 K the interfacial states contribution should dominate to this mechanism.

Above 330 K, the strength $\Delta\varepsilon'$ of the relaxation IV gradually increases and this leads (Fig. 7) to the decreasing of the total depletion width up to a value of about 150 nm at 370 K. This indicates, according to Eq. (10), that the density of interfacial states $n_t$ decreases and this leads to the increasing of its energy level, making the contribution of interfacial states less important as the temperature rises. On the other hand, the energy level of relaxation IV is in agreement with the estimate given by Alim et al. [19] for the barrier height of the grain boundary space charges formation under low DC electric field. Here it must be noted that the relaxation IV presents a maximum frequency peak close to 1 Hz. This means that the DRS measurements of this relaxation process are quasi-static measurements. Under the application of low frequencies electric field, the electrons crossed over the forward side barrier and flow into the grain boundary layers. These electrons fill into the empty electron traps. This filling should increase as the temperature rises, in order to justify the increasing of strength $\Delta\varepsilon'$ with the temperature. Therefore, space charges are formed at the grain boundary layers. According to Alim et al. [19] these space charges can easily overcome the reverse side barrier from some energy state and cross into the conduct band under the low electric field. The barrier height for these charges is found to be smaller than 0.2 eV. Hence, if we imagine the direction of the applied electric field from right to left, the electrons cross from the left conduction band to right hand side one, into the grain boundary filling the empty electron traps. Simultaneously de-trapping electrons flow into the right conduction band, and reverse. This polarization procedure suggested above, leads to the relaxation IV which observed at low frequency region.

## 4. Conclusions

The dielectric response of commercial low voltage ZnO varistors is studied in the present work, with the use of DRS and TSDC techniques in a wide range of temperatures. Four relaxation processes were found to be present in frequency spectrum of complex dielectric constant in DRS measurements, while at the region of higher temperatures and low frequencies the DC conductivity contribution dominates.

The two faster relaxation mechanisms are related to known processes in ZnO varistor: one should be related to the doubly ionised zinc interstitial $Zn_i^{\bullet\bullet}$, while the other should be associated with the oxygen vacancy $V_o^{\bullet}$ of the ZnO bulk traps. From the other two relaxation mechanisms, the faster one is associated to the MWS polarization which should be related to the intergranular Bi-rich phase without to exclude the contribution of the varistor porosity.

The fourth relaxation mechanism (slower mechanism) is associated to the ZnO–ZnO grain boundaries regions. For temperatures below ~330 K, the interfacial states contribution dominates to this dispersion, while above ~330 K the contribution of the empty electron traps in the grain boundary layers dominates. Based on the VDR block model for the ZnO varistor a gradual reduction in the total depletion width is observed at 320–330 K. The gradual decreasing of the total depletion width is related to the gradual decreases of the interfacial states density above 320–330 K.

## References


[1] T.K. Gupta, Application of zinc oxide varistors, Journal of American Ceramic Society 73 (7) (1990) 1817–1840.

[2] D.R. Clarke, Varistor ceramics, Journal of American Ceramic Society 82 (3) (1999) 485–502.

[3] C.-H. Lu, N. Chyi, H.-W. Wong, W.-J. Hwang, Effects of additives and secondary phases on the sintering behavior of zinc oxide-based varistors, Materials Chemistry and Physics 62 (2) (2000) 164–168.

[4] M.A. Ramirez, M. Cilense, P.R. Bueno, E. Longo, J.A. Varela, Comparison of non-ohmic accelerated ageing of the ZnO- and $SnO_2$-based voltage dependent varistors, Journal of Physics D: Applied Physics 42 (2009) 015503.

[5] K. Eda, Zinc oxide varistors, IEEE Electrical Insulation Magazine 5 (6) (1989) 28–30.

[6] F. Greuter, Electrically active interfaces in ZnO varistors, Solid State Ionics 75 (C) (1995) 67–78.

[7] G.D. Mahan, L.M. Levinson, H.R. Philipp, Theory of conduction in ZnO varistors, Journal of Applied Physics 50 (4) (1979) 2799–2812.

[8] G.E. Pike, Semiconductor grain-boundary admittance: theory, Physical Review B 30 (6) (1984) 795–802.

[9] M.A. Ramirez, A.Z. Simoes, P.R. Bueno, M.A. Marquez, M.O. Orlandi, J.A. Varela, Importance of oxygen atmosphere to recover the ZnO-based varistors properties, Journal of Materials Science 41 (19) (2006) 6221–6227.

[10] M. Elfwing, R. Osterlund, E. Olsson, Differences in wetting characteristics of $Bi_2O_3$ polymorphs in ZnO varistor materials, Journal of American Ceramic Society 83 (9) (2000) 2311–2314.

[11] A.K. Jonscher, Dielectric characterisation of semiconductors, Solid-State Electronics 33 (6) (1990) 737–742.

[12] F. Greuter, G. Blatter, Electrical properties of grain boundaries in polycrystalline compound semiconductors, Semiconductor Science Technology 5 (2) (1990) 111–137.

[13] A.M.R. Jiaping Han, P.Q. Senos, Mantas, Deep donors in polycrystalline Mn-doped ZnO, Materials Chemistry and Physics 75 (1–3) (2002) 117–120.

[14] Choom-W. Nahm, Effect of dopant (Al, Nb, Bi, La) on varistor properties of $ZnO–V_2O_5–MnO_2–Co_3O_4–Dy_2O_3$ ceramics, Ceramics International 36 (2010) 1109–1115.

[15] Y.W. Hong, J.H. Kim, The electrical properties of $Mn_3O_4$-doped ZnO, Ceramics International 30 (7) (2004) 1301–1306.

[16] Y.W. Hong, J.H. Kim, Impedance and admittance spectroscopy of $Mn_3O_4$-doped ZnO incorporated with $Sb_2O_3$ and $Bi_2O_3$, Ceramics International 30 (7) (2004) 1307–1311.

[17] S. Li, P. Cheng, J. Li, L. Zhao, Investigation on defect structure in ZnO varistor ceramics by dielectric spectra, in: Proceedings of IEEE International Conference on Solid Dielectric ICSD, 2007, pp. 207–210.

[18] J.A.M. AbuShama, S.W. Johston, R.S. Crandall, R. Noufi, Meyer–Neldel rule and the influence of entropy on capture cross-section determination in $Cu(In,Ga)Se_2$, Applied Physics Letters 87 (12) (2005) 123502.

[19] M.A. Alim, S. Li, F. Liu, P. Cheng, Electrical barriers in the ZnO varistor grain boundaries, Physica Status Solidi (A) 203 (2) (2006) 410–427.

[20] Y. Ohbuchi, T. Kawahara, Y. Okamoto, J. Morimoto, Distributions of interface states and bulk traps in ZnO varistors, Japanese Journal of Applied Physics 40 (1) (2001) 213–219.

[21] J. Tanaka, S. Hishita, Deep levels near the grain boundary in a zinc oxide varistor: energy change due to electrical degradation, Journal of American Ceramic Society 73 (5) (1990) 1425–1428.

[22] C. Tsonos, A. Kanapitsas, D. Triantis, C. Anastasiadis, I. Stavrakas, P. Pissis, Low temperature dielectric relaxations in ZnO varistors, Japanese Journal of Applied Physics 49 (5) (2010) 051102.

[23] C. Tsonos, L. Apekis, C. Zois, G. Tsonos, Microphase separation in ion-containing polyurethanes studied by dielectric measurements, Acta Materialia 52 (5) (2004) 1319–1326.

[24] J. Vanderschueren, J. Gasiot, in: P. Braunlich (Ed.), Thermally Stimulated Relaxation in Solids Topics in Applied Physics, vol. 37, Springer-Verlag, Berlin, 1980, p. 205.

[25] C.J.F. Bottcher, P. Bordewijk, Theory of Electric Polarization, vol. II, Elsevier, 1978,, p. 72.

[26] D. Fernandez Hevia, A.C. Caballero, J. de Frutos, J.F. Fernandez, Dominance of deep over shallow donors and the non-Debye response of ZnO-based varistors, Journal of European Ceramic Society 25 (12) (2005) 3005–3009.

[27] G. Garcia-Belmonte, J. Bisquert, F. Fabregat-Santiago, Effect of trap density on the dielectric response of varistor ceramics, Solid-State Electronics 43 (12) (1999) 2123–2127.

[28] C. Tsonos, L. Apekis, K. Viras, L. Stepanenko, L. Karabanova, L. Sergeeva, Electrical and dielectric behavior in blends of polyurethane-based ionomers, Solid State Ionics 143 (2) (2001) 229–249.

[29] P.R. Bueno, J.A. Varela, E. Longo, $SnO_2$, ZnO and related polycrystalline compound semiconductors: an overview and review on the voltage-dependent resistance (non-ohmic) feature, Journal European Ceramic Society 28 (3) (2008) 505–529.

[30] K. Boer, Survey of Semiconductor Physics, Van Nostrand Reinhold, New York, 1990.

[31] J. Li, B. Li, D. Zhai, S. Li, M.A. Alim, Dielectric response on the critical breakdown field in ZnO varistors, Journal of Physics D: Applied Physics 39 (23) (2006) 4969–4974.

[32] K.C. Kao, Dielectric Phenomena in Solids with Emphasis on Physical Concepts of Electronic Processes, Elsevier Academic Press, 2004, p. 430.

[33] J.P. Gambino, W.D. Kingery, G.E. Pike, H.R. Philipp, L.M. Levinson, Grain boundary electronic states in some simple ZnO varistors, Journal of Applied Physics 61 (7) (1987) 2571–2574.

[34] Y. Ohbuchi, J. Yoshino, Y. Okamoto, J. Morimoto, Evaluation of interface states in ZnO varistors by spectral analysis of deep level transient spectroscopy, Japanese Journal of Applied Physics 38 (2A) (1999) 899–900.

[35] G. Zang, J. Zhang, P. Zheng, J. Wang, C. Wang, Grain boundary effect on the dielectric properties of $CaCu_3Ti_4O_{12}$ ceramics, Journal of Physics D: Applied Physics 38 (11) (2005) 1824–1827.

[36] D.C. Look, D.C. Reynolds, J.R. Sizelove, R.L. Jones, C.W. Litton, G. Cantwell, W.C. Harsch, Electrical properties of bulk ZnO, Solid State Communications 105 (6) (1998) 399–401.